Aalborg Universitet

Accurate Temperature-Dependent IGBT Model for Predicting Commutation Voltage Overshoot in MW-level Power Converters

Sangwongwanich, Ariya; Iannuzzo, Francesco; Wu, Rui; Hygum, Morten; Blaabjerg, Frede

Published in:
Proceeding of 2020 IEEE Energy Conversion Congress and Exposition (ECCE)

DOI (link to publication from Publisher):
10.1109/ECCE44975.2020.9236305

Publication date:
2020

Document Version
Early version, also known as pre-print

Link to publication from Aalborg University

Citation for published version (APA):
Sangwongwanich, A., Iannuzzo, F., Wu, R., Hygum, M., & Blaabjerg, F. (2020). Accurate Temperature-Dependent IGBT Model for Predicting Commutation Voltage Overshoot in MW-level Power Converters. In *Proceeding of 2020 IEEE Energy Conversion Congress and Exposition (ECCE)* (pp. 3449-3455). Article 9236305 IEEE Press. https://doi.org/10.1109/ECCE44975.2020.9236305

General rights
Copyright and moral rights for the publications made accessible in the public portal are retained by the authors and/or other copyright owners and it is a condition of accessing publications that users recognise and abide by the legal requirements associated with these rights.

- Users may download and print one copy of any publication from the public portal for the purpose of private study or research.
- You may not further distribute the material or use it for any profit-making activity or commercial gain
- You may freely distribute the URL identifying the publication in the public portal -

Take down policy
If you believe that this document breaches copyright please contact us at vbn@aub.aau.dk providing details, and we will remove access to the work immediately and investigate your claim.

Downloaded from vbn.aau.dk on: December 06, 2025

Accurate Temperature-Dependent IGBT Model for Predicting Commutation Voltage Overshoot in MW-level Power Converters

Ariya Sangwongwanich*, Francesco Iannuzzo*, Rui Wu†, Morten Hygum†, and Frede Blaabjerg*
*Department of Energy Technology, Aalborg University, Aalborg, Denmark
†Vestas Wind Systems A/S, Aarhus, Denmark
ars@et.aau.dk

***Abstract*—Insulated-Gate Bipolar Transistor (IGBT) commutation voltage overshoot is a key design consideration for power stacks, especially in high-power applications. Conventionally, several double-pulse tests are required to map the over-voltage stress on the IGBT under different operating conditions, e.g., current loading and temperature, which is time- and resource-consuming. Thus, this paper proposes a physics-based IGBT model, which can be used for predicting the commutation voltage overshoot for MW-level power converters through simulation. The proposed IGBT model is based on a lumped-charge approach, where the temperature-dependent behavior of the IGBT is taken into consideration. A step-by-step model parameters identification process is also provided. The accuracy of the proposed IGBT model has been validated by comparing the predicted results with the experimental results under various operating conditions and achieving an error well below 2 %.**

***Index Terms*—Insulated-gate bipolar transistor (IGBT), lumped-charge model, physical model, temperature, robustness.**

I. Introduction

Reliability and robustness are important aspects of the power converter, especially in high-power applications (e.g., MW-level power converters) [1]. For the robust design of power stacks, the IGBT commutation voltage overshoot is a key design consideration. The MW-level power stack normally utilizes a busbar for the electrical connection. During the IGBT commutation (e.g., turn-off), the voltage overshoot will occur due to the parasitic inductance L_{dc}, as illustrated in Fig. 1 [2]–[4]. In order to ensure a robust design of the IGBT, a certain design margin between the maximum voltage overshoot and the IGBT blocking voltage capability needs to be allocated [1]. Conventionally, this is done through multiple testing conditions, where a double-pulse test is applied to the power stack under various current loading and operating temperature conditions to map the commutation voltage overshoot under various operating conditions [5]. However, this approach requires intensive testing, which is time-consuming and usually it slows down the product development cycle.

An alternative solution is to use a model-based approach to predict the overshoot voltage through simulations [6]. This approach offers a more time- and resource-effective solution, where minimum testing efforts are required. In order to be able to simulate the switching dynamics of the IGBT during the commutation, a physics-based IGBT model is required. While

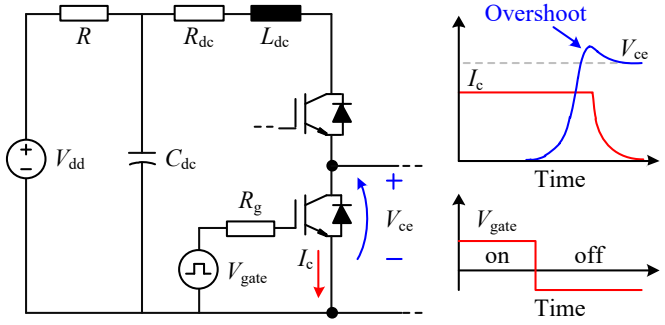

Fig. 1. Power stack circuit and the commutation voltage overshoot during IGBT turn-off due to the parasitic inductance L_{dc}.

several physics-based IGBT models (e.g., SPICE model) are available for low-power IGBTs [7], a very limited number of models have been developed for high-power applications, as they are either very complex or incur in terms of convergence issues. To solve this problem, a lumped-charge model has been proposed for high-voltage/high-power IGBTs in [8], [9], where the dynamic switching behavior of the IGBT was accurately modeled. However, the original lumped-charge model did not include the temperature-dependency behavior of the IGBT. Thus, it cannot accurately predict the commutation voltage overshoot of the IGBT under a wide range of operating temperature conditions, which is normally the case in the power stack in real applications.

Moreover, the lumped-charge IGBT model requires proper model parameters identification method for both the static and dynamic characteristics. In general, the parameters of the IGBT model can either be obtained from the datasheet of the IGBT or the experimental test [10]–[12]. However, without a proper model parameters identification process, a large number of iterations are usually required until both the static and dynamic characteristics of the lumped-charge IGBT model can be matched, especially under various operating temperature conditions [13], [14]. This parameters identification complexity limits the benefit of the physics-based IGBT model in practical applications. Therefore, a step-by-step model parameters identification guideline is required, which has not been addressed in previous research.

In this paper, a new physics-based IGBT model is presented, where a temperature-dependent lumped-charge approach is proposed in order to achieve a more resource-effective analysis tool for the robust design of the power stack. The rest of this paper is organized as follows: the description of a physics-based lumped-charge IGBT model is provided in Section II. Then, a step-by-step model parameters identification process is presented in Section III, which includes the pre-calculated parameters and the tuning of static and dynamic performance of the IGBT model. In Section IV, the model accuracy is validated by comparing the simulation results with the experiments. The results have demonstrated that the proposed model can predict the overshoot voltage of the IGBT over a wide range of operating conditions with errors below 2 %. The application of the proposed model with the parameter sensitivity analysis is also demonstrated in Section V. Finally, concluding remarks are provided in Section VI.

II. Physics-based Lumped-Charge IGBT Model

In the lumped-charge model, the IGBT is modeled by subdividing into several regions. Each region is then characterized by constant doping and/or carrier lifetime [8]. The behavior of each device region is characterized by the charges $q_{\mathrm{p,i}}$, which are the minority carrier concentrations and it is normalized to the volume of the region as

$$q_{\mathrm{p,i}} = q \cdot A \cdot w_{\mathrm{i}} \cdot p(i) \tag{1}$$

where q is the electron charge, A is the area, w_{i} is the thickness of the region and $p(i)$ is the concentration of minority carriers at the point i. Then, the boundary conditions of each region follow the junction law and the mass action together with the Kirchhoff's laws.

The lumped-charge IGBT model is subdivided into two parts: 1) Bipolar subcircuit and 2) Unipolar subcircuit, as it is illustrated in Fig. 2. The description of each part will be discussed in the following, while more details of the lumped-charge IGBT model can be found in [8]:

A. Bipolar Part of the Model

The bipolar part of the model represents the collector, base, body, and emitter regions of the IGBT. For the base and body regions, the current generators are implemented between the two adjacent nodes, e.g., i and j, to represent the hole current $i_{\mathrm{p,ij}}$ and the electron current $i_{\mathrm{n,ij}}$ as in the following:

$$\begin{cases} i_{\mathrm{p,ij}} &= \dfrac{q_{\mathrm{p,i}} - q_{\mathrm{p,j}}}{T_{\mathrm{p,ij}}} + \dfrac{q_{\mathrm{p,j}}}{T_{\mathrm{p,ij}}} \cdot \dfrac{v_{\mathrm{ij}}}{v_{\mathrm{T}}} \\ i_{\mathrm{n,ij}} &= \dfrac{q_{\mathrm{p,j}} - q_{\mathrm{p,i}}}{T_{\mathrm{n,ij}}} + \dfrac{q_{\mathrm{p,j}} + Q_{\mathrm{M,j}}}{T_{\mathrm{n,ij}}} \cdot \dfrac{v_{\mathrm{ij}}}{v_{\mathrm{T}}} \end{cases} \tag{2}$$

where $T_{\mathrm{p,ij}}$ and $T_{\mathrm{n,ij}}$ are the hole and electron transit time between nodes i and j, v_{ij} is the voltage drop between node i and j, v_{T} is the thermal voltage, and $Q_{\mathrm{M,j}}$ is the normalized majority concentration at node i.

In this work, the total of four current generators are placed, where the circuit model can be subdivided into two branches following the flow of hole and electron currents, as it is illustrated in Fig. 2.

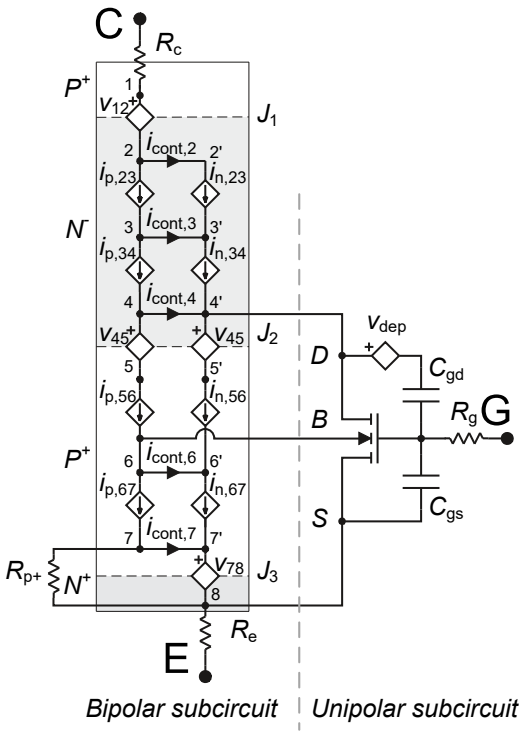

Fig. 2. Lumped-charge model of the used IGBT [8].

B. Unipolar Part of the Model

The unipolar part of the IGBT model includes the MOSFET model, which injects the electron current into the bipolar part. The turn-on and turn-off of the device can be controlled by the gate voltage. The non-linear dynamic behavior of the MOSFET is represented by a series voltage-controlled generator and the capacitance. The voltage-controlled generator can be implemented with the following expression:

$$V_{\mathrm{dep}} = \begin{cases} V_{\mathrm{DG}} + V_{\mathrm{n}}\Big(1 - \sqrt{1 + \dfrac{V_{\mathrm{DG}}}{V_{\mathrm{n}}}}\Big), & \text{when} \quad V_{\mathrm{DG}} \geq 0 \\ 0, & \text{when} \quad V_{\mathrm{DG}} < 0 \end{cases} \tag{3}$$

where V_{n} is a normalization factor, which is dependent on the doping and V_{DG} is the drain-gate voltage of the MOSFET.

III. Proposed IGBT Model Parameters Identification Method

The proposed model parameters identification method consists of three main parts: 1) Pre-calculated parameters, 2) Tuning of static performance, and 3) Tuning of dynamic performance. The overall model parameters identification process is illustrated in Fig. 3, and it will be discussed in the following.

A. Pre-calculated Parameters

First, a certain set of parameters for the lumped-charge IGBT model can be obtained from the key electrical parameters of the IGBT, which are normally provided in the datasheet. This includes the rated (continuous DC) collector

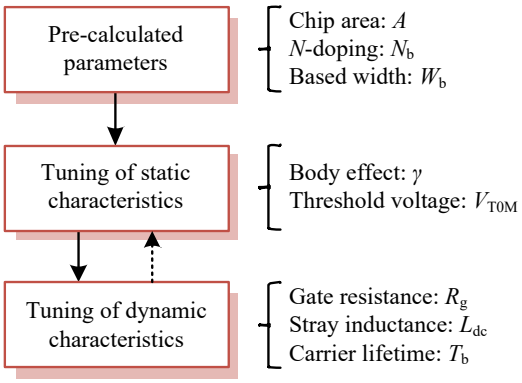

Fig. 3. Overall workflow diagram of the proposed IGBT model parameters identification process.

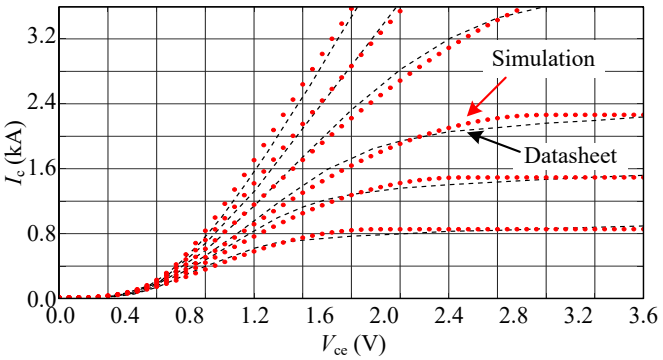

Fig. 4. Output characteristic of IGBT at different gate voltage biases V_{ge} conditions.

current I_{cnom} and the rated blocking voltage V_{CES} of the IGBT. These parameters are used for determining the chip area A, doping concentration of the N-region N_b, and the width of the base region W_b of the IGBT as given in the following:

1) Chip Area A:

$$A = \frac{I_{cnom}}{J_{tn}} \tag{4}$$

where J_{tn} is the current density. Alternatively, the chip area can also be measured physically (if it is accessible).

2) Doping Concentration of the N-Region N_b:

$$N_b = \frac{(E_{crit})^2 \cdot \varepsilon}{2 \cdot V_{CES} \cdot q} \tag{5}$$

where E_{crit} is the critical electric field, q is the electron charge, and ε is the permittivity of the material.

3) Width of the base region W_b:

$$W_b = \frac{2 \cdot V_{CES}}{E_{crit}} \tag{6}$$

B. Tuning of Static Performance

The static performance of the IGBT model needs to be tuned to match the datasheet (or experimental) data. First, the output characteristic of the IGBT needs to be tuned at different gate voltage biases V_{ge}. This static characteristic determines the relationship between the on-state voltage drop of the IGBT V_{ce} at a given collector current I_c and at different gate voltage biases V_{ge}, as it is shown in Fig. 4. This characteristic is mainly dictated by the Transconductance parameter K_{pm}, which determines the slope of the curve following:

1) Transconductance Parameter K_{pm}:

$$K_{pm} = \begin{cases} \dfrac{I_c}{(V_{ge} - V_{th})V_{ce} - \frac{1}{2}V_{ce}^2}, & \text{when} \quad V_{ge} - V_{th} > V_{ce} \\ \dfrac{2I_c}{(V_{ge} - V_{th})^2}, & \text{when} \quad V_{ge} - V_{th} \leq V_{ce} \end{cases} \tag{7}$$

where V_{th} is the threshold voltage of the IGBT.

Then, the output characteristic of the IGBT needs to be tuned at different operating temperatures T_{vj}, as it is shown in Fig. 5. This static characteristic determines the relationship between the on-state voltage drop of the IGBT at a given collector current and at different chip temperature. The parameter of the IGBT model that dictates this characteristic is the Body Effect coefficient γ, which should be temperature-dependent to represent the effect of the voltage drop at different temperature conditions following:

2) Body Effect Coefficient γ:

$$\gamma = \gamma_0 \left(\frac{273 + T_{vj}}{298} \right)^{k_1} \tag{8}$$

where γ_0 is the Body Effect coefficient at T_{vj} = 25 °C and k_1 is a scaling factor.

The transfer characteristic of the IGBT is another important static characteristic, which determines the relationship between the gate-emitter voltage of the IGBT V_{ge} at a given collector current I_c and at different chip temperatures T_{vj}, as it is shown in Fig. 6. This characteristic can be tuned through the zero-bias threshold voltage V_{T0M}, which is also needed to be modeled as a temperature-dependent parameter following:

3) Zero-bias Threshold Voltage V_{T0M}:

$$V_{T0M} = V_{T0M0} \left(\frac{273 + T_{vj}}{298} \right)^{k_2} \tag{9}$$

where V_{T0M0} is the zero-bias threshold voltage at T_{vj} = 25 °C and k_2 is a scaling factor.

C. Tuning of Dynamic Performance

The tuning of the IGBT dynamic performance requires experimental tests (e.g., double-pulse testing), where the IGBT model can be tuned by comparing the double-pulse test results between the experiments and simulations. However, in this case, only two experimental double-pulse tests at the maximum and minimum operating temperature conditions are required, which minimizes the testing efforts.

First, the turn-off switching behavior at one of the operating temperatures (e.g., at T_{vj} = 25 °C) is used for determining the nominal value of: 1) Gate resistance R_{g0}, which affects the

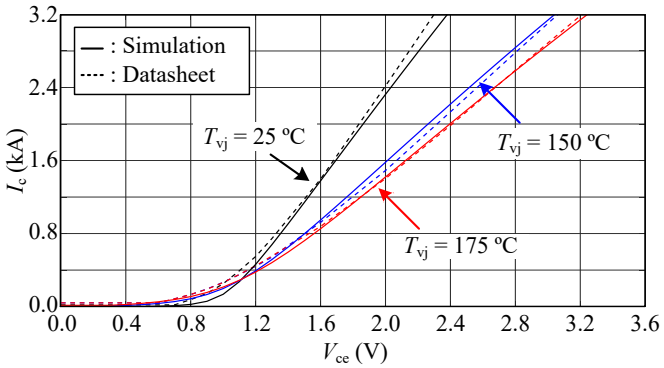

Fig. 5. Output characteristic of IGBT at different operating temperature T_{vj} conditions.

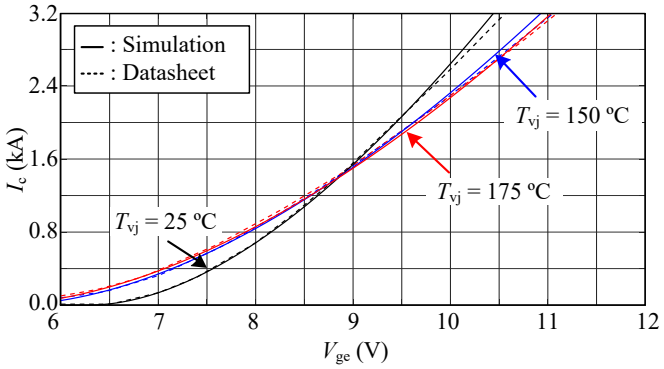

Fig. 6. Transfer characteristic of IGBT at different operating temperature T_{vj} conditions.

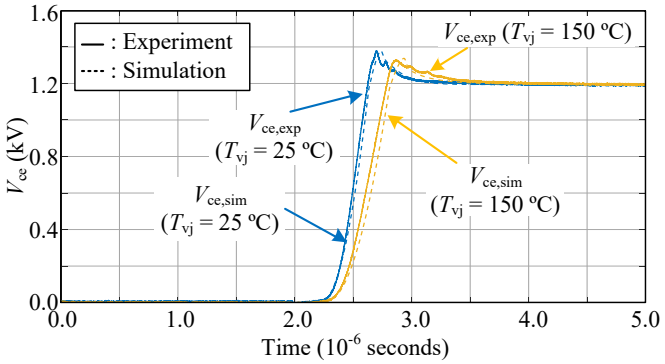

Fig. 7. Experiment (exp) and simulation (sim) of the collector-emitter voltage V_{ce} during turn-off at different temperature T_{vj}.

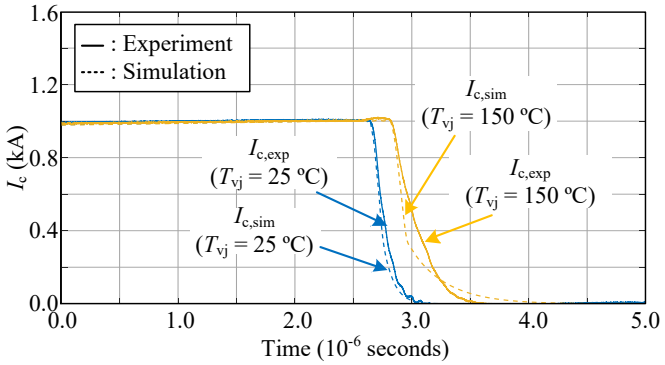

Fig. 8. Experiment (exp) and simulation (sim) of the collector-emitter current I_c during turn-off at different temperature T_{vj}

turn-off delay time and the slope of the collector-emitter voltage V_{ce}, 2) Stray inductance L_{dc} (i.e., busbar and parasitic inductance), which affects the voltage overshoot, and 3) Carrier lifetime T_{b0}, which affects the tail current of the IGBT during turn-off. The results during the IGBT turn-off commutation at T_{vj} = 25 °C are shown in Figs. 7 and 8, where the simulation results are compared with the experiments. Afterwards, the experimental test at another operating temperature (e.g., at T_{vj} = 150 °C) is used for modeling the temperature-dependent behavior of the gate resistance R_g and carrier lifetime T_b.

The delay time and the slope of the collector-emitter voltage during turn-off characteristics are strongly temperature-dependent. In order to include this dependency in the model, the (internal) gate resistance should be modeled with a temperature-dependent value following:

1) Gate Resistance R_g:

$$R_g = R_{g0} + \Delta R(T_{vj} - 25) \tag{10}$$

where R_{g0} is gate resistance at T_{vj} = 25 °C and ΔR is the change in the resistance with temperature.

Similarly, the tail current characteristic of the IGBT is strongly dependent on the temperature condition of the device. In order to include this behavior in the model, the carrier lifetime of the IGBT T_b needs to be modeled as a temperature-dependent parameter. According to the literature [7], the temperature-dependent carrier lifetime T_b can be modeled as the following:

2) Carrier Lifetime T_b:

$$T_b = T_{b0}\left(\frac{273 + T_{vj}}{298}\right)^{k_3} \tag{11}$$

where T_{b0} is the carrier lifetime at T_{vj} = 25 °C and k_3 is a scaling factor.

By modeling the above parameters with temperature-dependent behavior, the dynamic performance during the turn-off of the IGBT under different operating temperatures can be captured, as it is shown in Figs. 7 and 8. Notably, the static characteristics need to be verified after the dynamic characteristics are tuned. In some cases, one more iteration is required to re-adjust the static performance parameters with the same procedure as previously discussed, and following the workflow diagram of Fig. 3.

IV. Model Accuracy Validation (Experiments)

The simulation results during voltage commutation (i.e., turn-off) are compared with the experimental results under various operating conditions to validate the model accuracy. A commercially-available 1700V/1800A IGBT is considered as a case study [15]. The lumped-charge IGBT model parameters

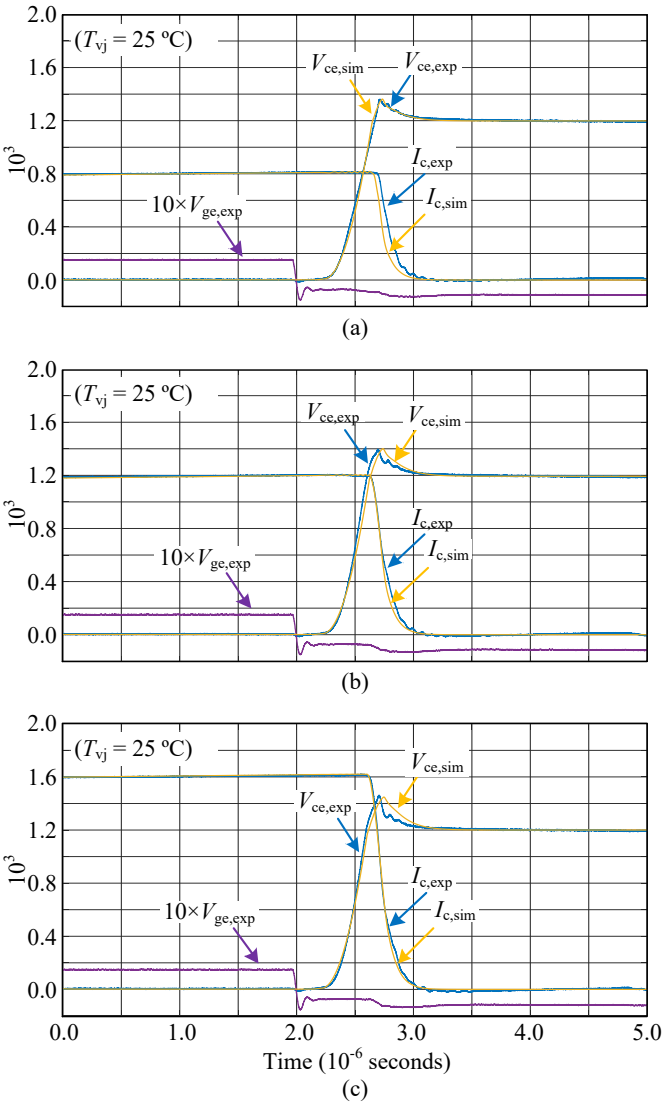

Fig. 9. Experiment (exp) and simulation (sim) of IGBT turn-off switching transition under the loading current I_c of: a) 800 A, b) 1000 A, and c) 1600 A (T_{vj} = 25 °C).

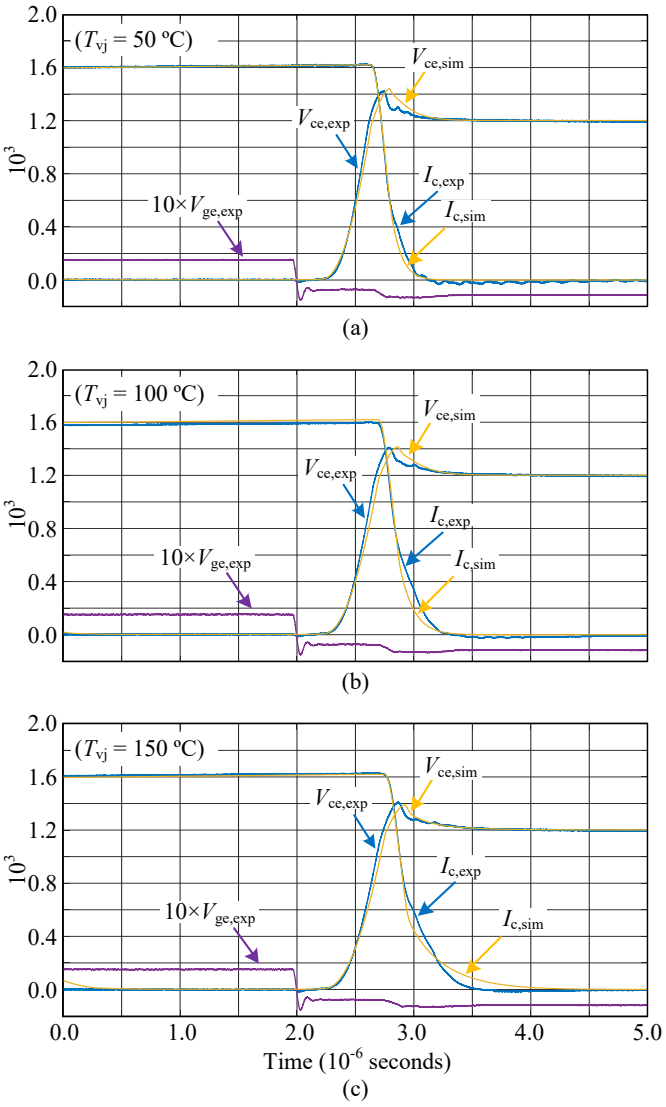

Fig. 10. Experiment (exp) and simulation (sim) of IGBT turn-off switching transition under the operating temperature T_{vj} of: a) 50 °C, b) 100 °C, and c) 150 °C (I_c = 1600 A).

identification has been carrier out based on the datasheet and the double-pulse test at only two operating conditions: 1) I_c = 1000 A, T_{vj} = 25 °C and 2) I_c = 1000 A, T_{vj} = 150 °C.

A. Load Current Variation

A load current of the IGBT between I_c = 400 A and I_c = 1800 A is considered during the test, while the operating temperature is T_{vj} = 25 °C. The switching waveforms during turn-off commutation are shown in Fig. 9(a), where the experimental and simulation results at I_c = 800 A are demonstrated. It can be seen from the results that the dynamic switching behavior of the IGBT can be accurately predicted with the proposed model. This can be seen from the slope of the voltage and current as well as the overshoot voltage during the commutation. The other operating conditions at I_c = 1200 A and I_c = 1600 A are shown in Figs. 9(b) and 9(c), respectively. It can be noticed from the case where I_c = 1200 A and I_c = 1600 A that the overshoot voltage during the commutation increases (compared to the case with I_c = 800 A) due to an increase in the collector current and its derivative (dI_c/dt). Nevertheless, the proposed model can also accurately model the turn-off behavior over a wide range of load current conditions, where the overshoot voltage during the commutation is very closely matched with the experiment.

B. Operating Temperature Variation

The accuracy of the proposed model is also validated under different operating temperature conditions, as it is shown in Fig. 10. The experimental tests have been carried out by varying the operating temperature from T_{vj} = 25 °C to T_{vj} = 150 °C while the load current is kept at I_c = 1600 A. From

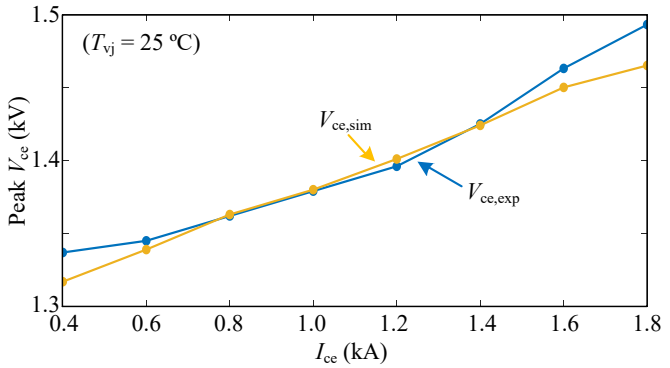

Fig. 11. Overshoot voltage under different loading currents I_c, where $V_{ce,sim}$ and $V_{ce,exp}$ denote the simulation and experimental results, respectively.

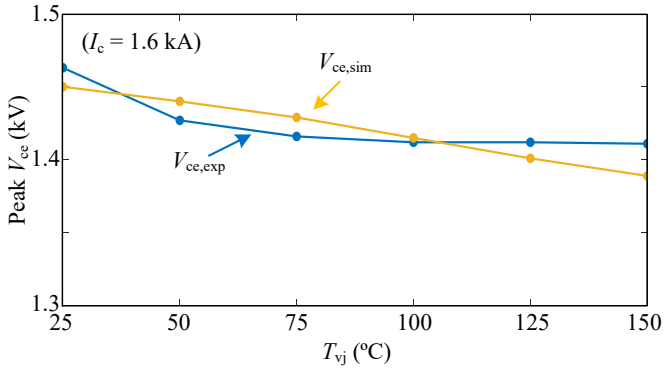

Fig. 12. Overshoot voltage under different operating temperatures T_{vj}, where $V_{ce,sim}$ and $V_{ce,exp}$ denote the simulation and experimental results, respectively.

the switching waveforms under the operating temperature of T_{vj} = 50 °C, T_{vj} = 100 °C, and T_{vj} = 150 °C in Fig. 10, it can be noticed that the slope of I_c (and also V_{ce}) during the voltage commutation decreases as the operating temperature increases from T_{vj} = 50 °C to T_{vj} = 150 °C. As a consequence, the overshoot voltage is decreased as the operating temperature is increasing. Moreover, the tail-current of the IGBT also increases at T_{vj} = 150 °C. The proposed IGBT model can predict these behaviors accurately, where the simulation results agree well with the experiments.

C. Result Summary

The overshoot voltage (i.e., peak V_{ce}) under different load current I_c and operating temperature T_{vj} conditions are summarized in Figs. 11 and 12, respectively. In general, the overshoot voltage increases as the load current increases. This is mainly due to the increase in the dI_c/dt at the higher load currents following the results in Fig. 11. According to the results, the overshoot voltage can be accurately predicted over a wide range of load current conditions. The maximum error in the overshoot voltage prediction is 28 V (i.e., 1.89 %) which occurs when I_c = 1800 A. In contrast, the overshoot voltage decreases when the operating temperature increases, as it is shown in Fig. 12. At the high operating temperature (e.g., T_{vj} = 150 °C), the overshoot voltage decreases since the IGBT switching dynamic is slower (e.g., lower switching speed) and thus lower dI_c/dt. In this case, the maximum error is 22 V (i.e., 1.56 %), which is when T_{vj} = 150 °C.

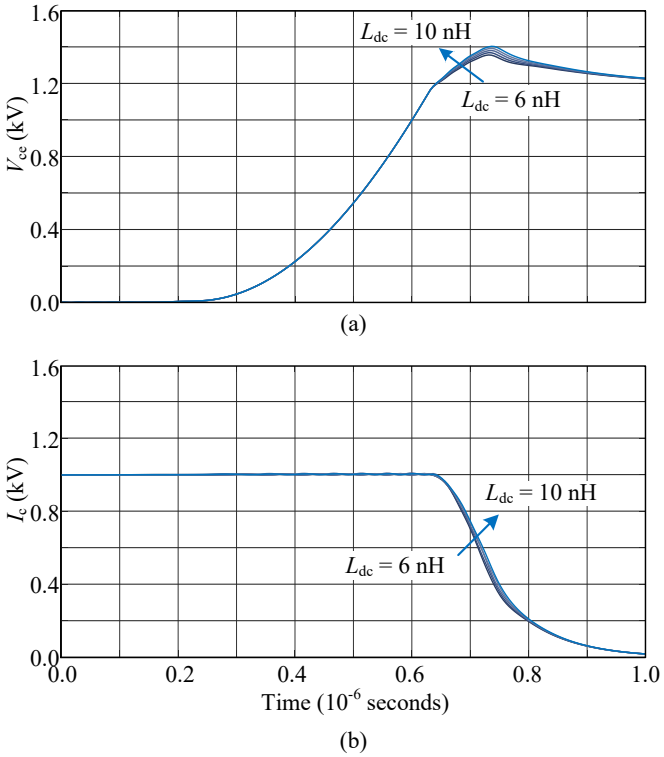

Fig. 13. Turn-off transition of the IGBT (simulation) with different stray inductance L_{dc} values: (a) collector-emitter current I_c and (b) collector-emitter voltage V_{ce}.

V. Parameter Sensitivity Analysis

Another advantage of the model-based overshoot voltage prediction approach is its ability to analyze the uncertainty due to parameter variations, which usually occur in practical applications. In this section, the parameter sensitivity analysis is carried out with the proposed model, where the variations in the stray inductance of the busbar L_{dc} and the gate resistance R_g are taken into consideration.

A. Stray Inductance of the Busbar

The stray inductance of the busbar L_{dc}, in many cases, varies in a certain range from one power stack to another. Therefore, it is important to analyze the sensitivity of the overshoot voltage due to the stray inductance variation. The overshoot voltage when the stray inductance value varies from L_{dc} = 6 nH to L_{dc} = 10 nH is demonstrated in Fig. 13. In this case, the overshoot voltage (i.e., the peak value of V_{ce}) varies from 1356 V to 1403 V. This indicates the robustness design margin which needs to be allocated due to the variation in the stray inductance of the busbar.

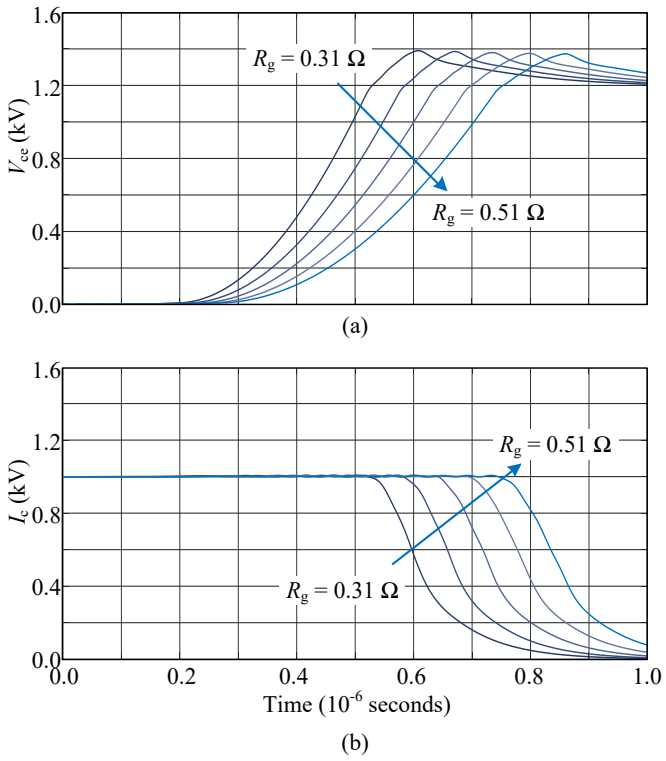

Fig. 14. Turn-off transition of the IGBT (simulation) with different gate resistance R_g values: (a) collector-emitter current I_c and (b) collector-emitter voltage V_{ce}.

B. Gate Resistance

The gate resistance value R_g may also vary to a certain range in practice. The impact of gate resistance variation on the overshoot voltage is demonstrated in Fig. 14, where the gate resistance value between R_g = 0.31 Ω and R_g = 0.51 Ω is considered. It can be seen from the results that the slope of the collector-emitter voltage V_{ce} changes significantly with the variation of the gate resistance. However, the overshoot voltage only varies from 1373 V to 1390 V. This indicates that the overshoot voltage is less sensitive with the gate resistance variation (compared to the stray inductance of the busbar). Nevertheless, the variation in the gate resistance will affect the other performance metrics such as power loss, which can also be analyzed with the proposed IGBT model.

VI. Conclusions

In this paper, a physics-based IGBT model which is capable of predicting the commutation overshoot voltage in a busbar is proposed. The proposed model is based on a lumped-charge one, which has been modified to include temperature dependence and thereby improve the model accuracy under a wide range of operating temperatures. A step-by-step model parameters identification process is also presented in this paper, where the tuning of static and dynamic performances of the IGBT model is discussed. The accuracy of the proposed model has been verified against experimental results under a wide range of load currents and operating temperature conditions. According to the results, the commutation overshoot voltage can be accurately predicted with the proposed model, where the maximum error in the prediction is below 2 %. The proposed model is very useful, e.g., for sensitivity analysis, where the impact of the parameter variation on the overshoot voltage can be investigated. This feature has been demonstrated by considering the parameter variation in the busbar stray inductance and the gate resistance.

Acknowledgment

This work was supported in part by Innovation Fund Denmark through the Advanced Power Electronic Technology and Tools (APETT) project and in part by the Reliable Power Electronic-Based Power System (REPEPS) project at the Department of Energy Technology, Aalborg University as a part of the Villum Investigator Program funded by the Villum Foundation.

References

[1] *Application Manual Power Semiconductors*, Semikron International GmbH, 2015, rev. 2.
[2] G. Busatto, C. Abbate, B. Abbate, and F. Iannuzzo, "IGBT modules robustness during turn-off commutation," *Microelectron. Reliab.*, vol. 48, no. 8-9, pp. 1435–1439, 2008.
[3] H. J. Beukes, J. H. R. Enslin, and R. Spee, "Busbar design considerations for high power IGBT converters," in *Proc. PESC97*, vol. 2, pp. 847–853, 1997.
[4] C. Chen, X. Pei, Y. Chen, and Y. Kang, "Investigation, evaluation, and optimization of stray inductance in laminated busbar," *IEEE Trans. Power Electron.*, vol. 29, no. 7, pp. 3679–3693, 2014.
[5] Z. Chen, D. Boroyevich, and R. Burgos, "Experimental parametric study of the parasitic inductance influence on MOSFET switching characteristics," in *Proc. IPEC-ECCE Asia*, pp. 164–169, 2010.
[6] J. Wang, H. S. Chung, and R. T. Li, "Characterization and experimental assessment of the effects of parasitic elements on the MOSFET switching performance," *IEEE Trans. Power Electron.*, vol. 28, no. 1, pp. 573–590, 2013.
[7] P. R. Palmer, E. Santi, J. L. Hudgins, X. Kang, J. C. Joyce, and P. Y. Eng, "Circuit simulator models for the diode and IGBT with full temperature dependent features," *IEEE Trans. Power Electron.*, vol. 18, no. 5, pp. 1220–1229, 2003.
[8] F. Iannuzzo and G. Busatto, "Physical CAD model for high-voltage IGBTs based on lumped-charge approach," *IEEE Trans. Power Electron.*, vol. 19, no. 4, pp. 885–893, 2004.
[9] Y. Duan, F. Xiao, Y. Luo, and F. Iannuzzo, "A lumped-charge approach based physical SPICE-model for high power soft-punch through IGBT," *IEEE J. Emerg. Sel. Topics Power Electron.*, vol. 7, no. 1, pp. 62–70, 2019.
[10] R. Withanage, N. Shammas, S. Tennakoon, C. Oates, and W. Crookes, "IGBT parameter extraction for the Hefner IGBT model," in *Proc. UPEC*, vol. 2, pp. 613–617, 2006.
[11] A. T. Bryant, X. Kang, E. Santi, P. R. Palmer, and J. L. Hudgins, "Two-step parameter extraction procedure with formal optimization for physics-based circuit simulator IGBT and p-i-n diode models," *IEEE Trans. Power Electron.*, vol. 21, no. 2, pp. 295–309, 2006.
[12] G. Sfakianakis, M. Nawaz, and F. Chimento, "A temperature dependent simple spice based modeling platform for power IGBT modules," in *Proc. ECCE*, pp. 2873–2879, 2014.
[13] D. Cavaiuolo, M. Riccio, G. De Falco, G. Romano, A. Irace, G. Breglio, D. Daprà, L. Merlin, R. Carta, C. Sanfilippo, and F. Crudelini, "An effective parameters calibration technique for PSpice IGBT models application," in *Proc. SPEEDAM*, pp. 133–138, 2014.
[14] C. G. Suarez, P. D. Reigosa, F. Iannuzzo, I. Trintis, and F. Blaabjerg, "Parameter extraction for PSpice models by means of an automated optimization tool - an IGBT model study case," in *Proc. PCIM Europe*, pp. 1–8, 2016.
[15] *FF1800R17IP5*, Infineon Technologies AG, Germany, 2017, rev. 3.2.